Evaluation and Selection of $LiNbO_3$ and $LiTaO_3$ Substrates for SAW Devices by the LFB Ultrasonic Material Characterization System

Jun-ichi Kushibiki, *Member, IEEE*, Yuji Ohashi, and Yuu Ono, *Member, IEEE*

***Abstract*—This paper demonstrates the evaluation and selection of commercially available $LiNbO_3$ and $LiTaO_3$ single crystals and wafers for surface acoustic wave (SAW) devices using the line-focus-beam ultrasonic material characterization (LFB-UMC) system. This system enables measuring leaky-SAW (LSAW) propagation characteristics precisely and efficiently for a number of specimens. The wafers are prepared from the top, middle, and bottom parts of four 128°YX $LiNbO_3$ and seven X-112°Y $LiTaO_3$ single crystals. For both series of crystals, the measured LSAW velocities increase from top to bottom in the crystals and with the increasing crystal growth number. The velocity changes for all wafers are 0.036% for 128°YX $LiNbO_3$ and 0.035% for X-112°Y $LiTaO_3$, corresponding to changes of 0.038 mol% and 0.075 mol% in Li_2O concentration, respectively. Moreover, the inhomogeneity in the first X-112°Y $LiTaO_3$ single crystal caused by some undesirable wafer fabrication processes can be detected precisely, although it is difficult for the conventional methods to obtain such information.**

I. Introduction

Ferroelectric single crystals of $LiNbO_3$ [1], [2] and $LiTaO_3$ [1], [3] have been widely used as substrates for various electronic devices because of their acoustic and optical properties valued in the field of engineering. Among the ultrasonic devices utilizing piezoelectricity, surface acoustic wave (SAW) devices are the most highly recognized. Production of single-crystal substrates with high elastic homogeneity is essential for developing high-performance SAW devices [4]. For research and development, a material characterization system with extremely high measurement accuracy is needed. Such a system must be able to detect slight changes of elastic properties in or among crystals and substrates and feed back information to improve the crystal growth conditions and substrate fabrication processes.

The authors have been studying the development and application of ultrasonic micro-spectroscopy (UMS) technology [5], [6], whose main system is the line-focus-beam (LFB) acoustic microscopy system [7]. This technology is able to analyze and evaluate materials through highly accurate, quantitative measurements or imaging measurements of the acoustic properties with nondestructive and noncontacting procedures. In characterizing $LiNbO_3$ and $LiTaO_3$ single-crystal substrates using the LFB acoustic microscopy system, elastic inhomogeneities in the substrates caused by the chemical composition ratio changes and the residual multi-domains, in particular, have been detected with high accuracy as the velocity changes of leaky SAWs (LSAWs) [8]–[12], a significant achievement that could not be accomplished by conventional methods. Frequent improvements of the system also have been made to increase its accuracy [13]. Recently, a new version of the system was developed. The new system has the capability of making highly accurate and efficient measurements for a number of wafers, which will be of great use in the practical application of the system [14]. One of the problems encountered in precise velocity measurements of thin substrate materials such as wafers is the apparent change of measured values due to the waves reflected from the back surface. Methods for eliminating these influences have been proposed and demonstrated [15]–[18].

In this paper, the LFB ultrasonic material characterization (UMC) system developed recently is applied to evaluate and select commercially available, 127.86° rotated Y-cut X-propagating (128°YX) $LiNbO_3$ [19] and X-cut 112.2° rotated Y-propagating (X-112°Y) $LiTaO_3$ [20] single crystals and wafers.

II. System

The LFB-UMC system utilizes ultrasonic line-focused waves and can measure the propagation characteristics (phase velocity and attenuation) of LSAWs excited and propagated along one desired direction on the water-loaded specimen surface. The measurement principle and the system were described in detail in the literature [7]. Fig. 1 shows the block diagram of the LFB system used in the demonstration measurements in this paper. With commercially available wafers, it is essential to measure a number of wafers efficiently in succession when evaluating elastic property distributions in the crystals and systematically detecting elastic property changes among the crystals. In this system, therefore, a temperature-controlled chamber is introduced to stabilize the temperature environment of the mechanical system as well as the ultrasonic device and specimens for a long period of time. In addition,

Manuscript received December 29, 1999; accepted February 11, 2000. This work was supported in part by Research Grants-in-Aid from the Ministry of Education, Science and Culture of Japan, from the Japan Society for the Promotion of Science for the Research for the Future Program, and from the Mitsubishi Foundation.

The authors are with the Department of Electrical Engineering, Tohoku University, Sendai 980-8579, Japan (e-mail: kushi@ecei.tohoku.ac.jp).

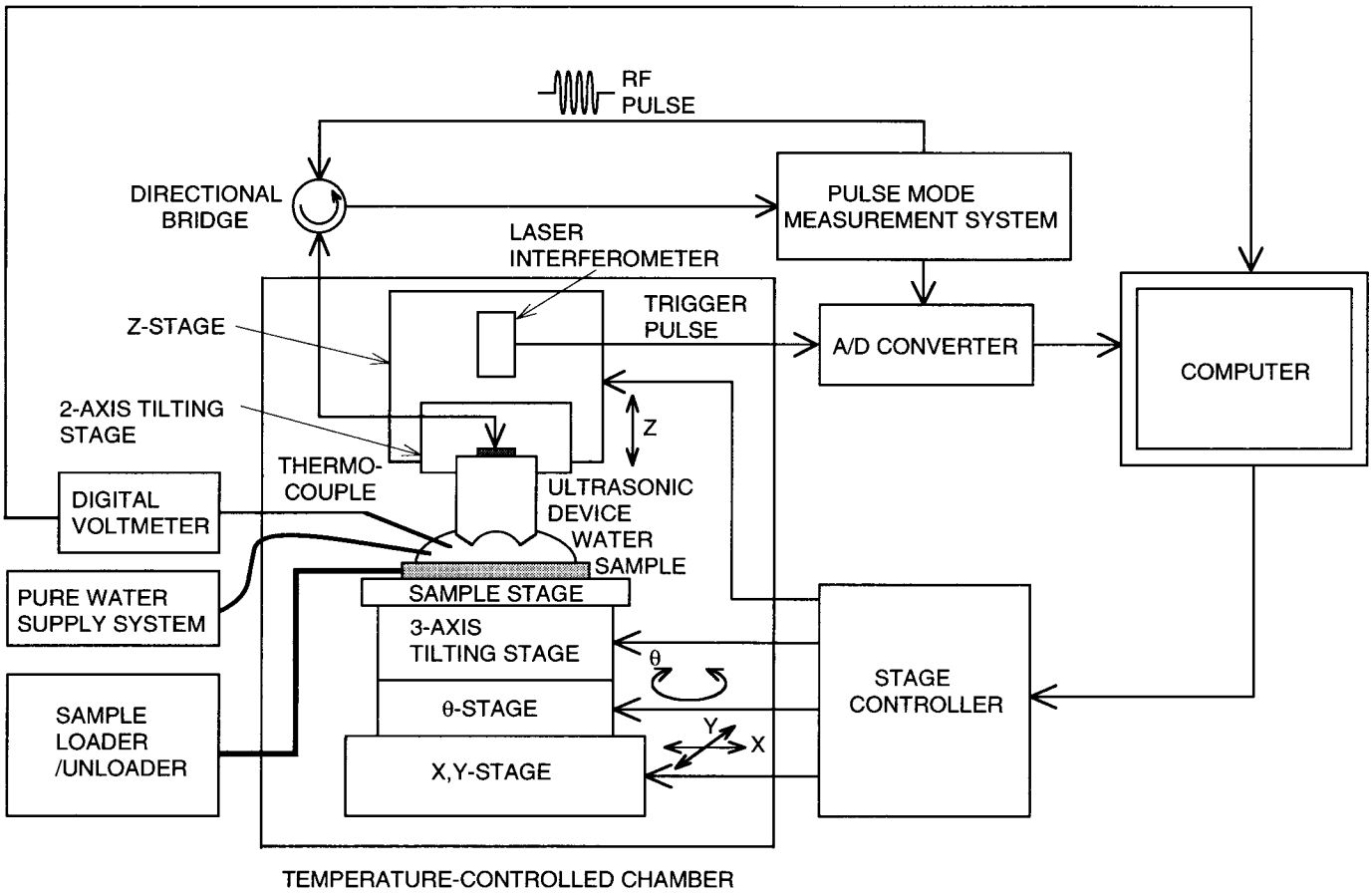

Fig. 1. Block diagram of the LFB ultrasonic material characterization system.

the system is equipped with a specimen transfer system, a temperature-controlled pure water supply system, and an automatic three-axis tilting stage to keep the chamber closed while loading and changing specimens, supplying the water couplant, and aligning the specimen and the ultrasonic device so that highly accurate measurements are made efficiently without disturbing the stabilized measurement environment. The system can measure LSAW velocity with a reproducibility of $\pm 0.0015\%$ ($\pm 2\sigma$: σ is the standard deviation) at a single chosen point and an absolute accuracy of around $\pm 0.01\%$ [14], [21].

III. Procedure

When the LFB system is applied to characterize thin specimens such as commercially available wafers, measurement errors might occur if the specimen thickness h does not satisfy the following equation:

$$h > V_\ell \cdot PW/2, \tag{1}$$

where V_ℓ is the velocity of longitudinal waves in the specimen, and PW is the radio frequency (RF) tone burst pulse width used for measurements. An RF pulse width of 500 ns is usually employed around 200 MHz using a sapphire cylindrical ultrasonic lens with a 1-mm radius. The back reflection effect must be considered for almost all the wafers for SAW devices because they are less than 0.5-mm thick. Also, the measurement errors due to the back reflection vary with the acoustic impedance of the solid specimen because the amplitude of the waves reflected from its back surface depends on the reflection and transmission coefficients at the front boundary between the water couplant and the solid specimen [18].

As a typical example of the back reflection effect on measured LSAW values, Fig. 2 shows the frequency dependences of LSAW velocities in the X-axis propagation direction measured on a 0.5-mm thick 128°Y-cut $LiNbO_3$ specimen, which does not satisfy (1), and a 3-mm thick specimen, which satisfies the condition. Apparent periodic changes due to back reflection are observed in the curve (solid line) for the thin specimen, which are not exhibited in the curve shown by the dotted line for the thick specimen. These apparent changes must be eliminated to obtain the intrinsic elastic information of the specimen. The variations observed in the dotted curve in Fig. 2 represent the frequency characteristics of the ultrasonic device and are to be corrected by the system calibration method [22].

With the preceding information, material characterization is conducted following the proper measurement procedure shown by the flow chart in Fig. 3. The thickness and longitudinal velocity of the specimen determine whether or not the back reflection causes erroneous measurement results. A measurement method is then chosen accordingly: the usual measurement method or the methods for elim-

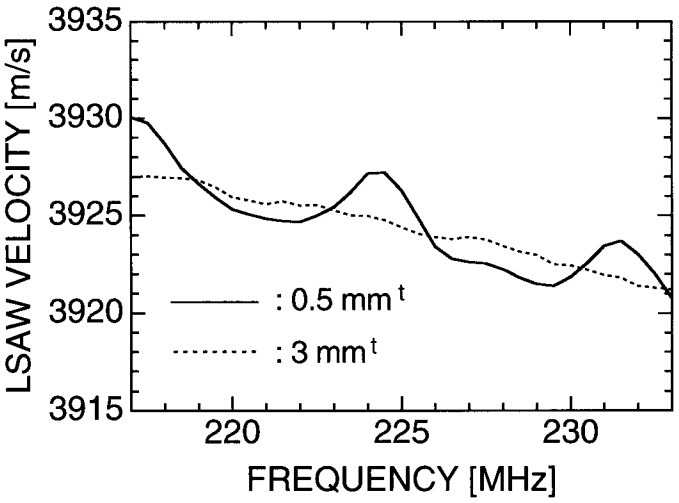

Fig. 2. Frequency dependences of LSAW velocities for 128°YX-$LiNbO_3$ substrates.

inating the back reflection influence proposed in the literature [18], which include reducing the RF pulse width, scattering acoustic waves from the roughened back surface, and taking the moving average of the frequency dependence of LSAW velocities. For specimens with thicknesses that do not satisfy (1), we should examine whether or not the back reflection affects the measured results, considering the roughness of the back surfaces and the acoustic impedance of the specimens. We then should determine whether or not the waves reflected from the back surfaces can be eliminated by reducing the RF pulse width to the lower limit $PW_{\min}$, below which the measurement accuracy deteriorates. If there is no back reflection effect, measurements are made with a usual or reduced RF pulse at or above $PW_{\min}$. When the back reflection influence is severe, the frequency characteristics of LSAW velocities are measured with a normal pulse width, and the moving average method is used to obtain measured values. If measurements are made at a larger number of points, the approximated correction method [17] also is applied for efficient measurements. The system calibration method using the standard specimen [22] then is applied to the measured values obtained by the methods described here, in order to obtain intrinsic LSAW velocities.

IV. Applications

A. Specimens

Specimens are commercially available, 3-inch 128°Y-cut $LiNbO_3$ and 4-inch X-cut $LiTaO_3$ single crystal wafers (Yamaju Ceramics Co., Seto, Japan, produced in 1989). Crystals were grown by the Czochralski (CZ) technique. In a commercial point of view to reduce the production costs, multiple crystals were repeatedly grown within a certain permissible composition variation for the crystal growths as a series of crystals in the same furnace, in which the crucible was recharged with the same amount of the starting

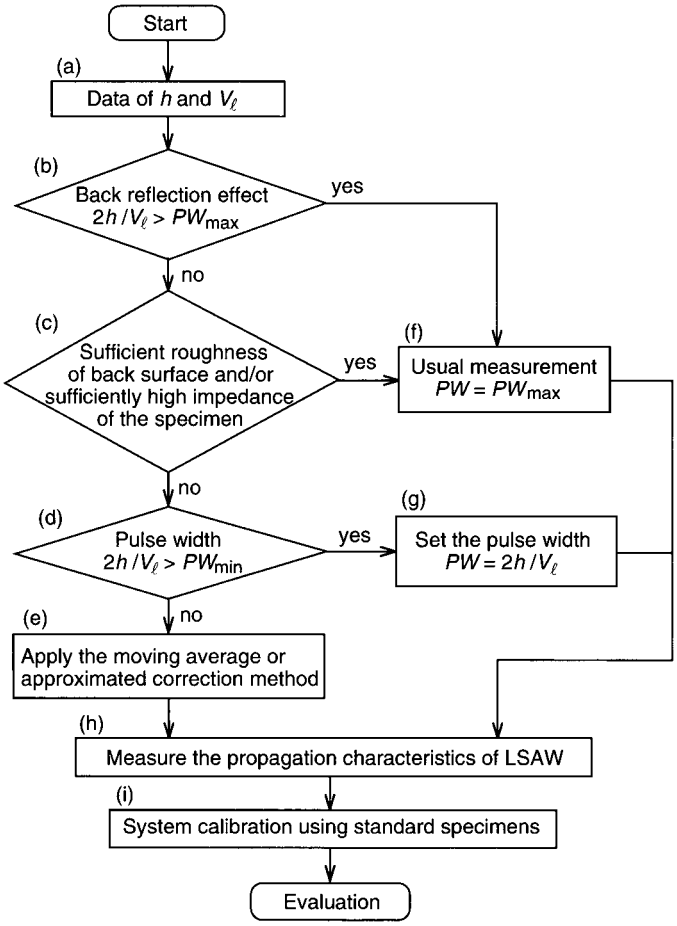

Fig. 3. Flow chart of measuring thin specimens by LFB system.

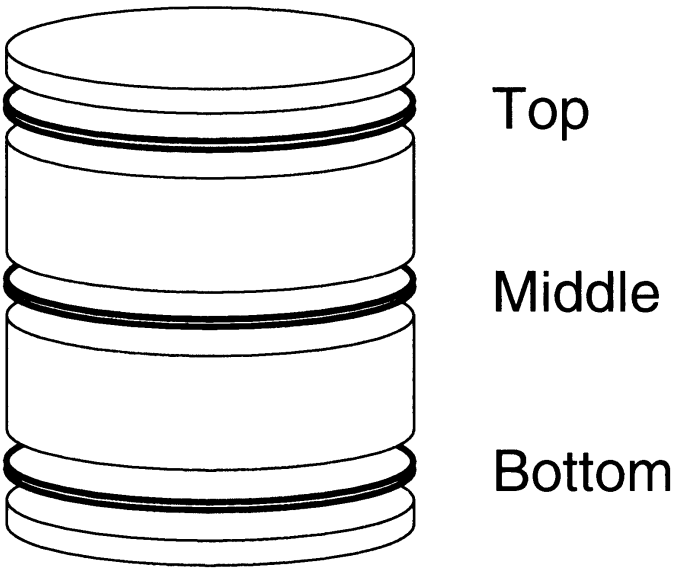

Fig. 4. Sample configuration.

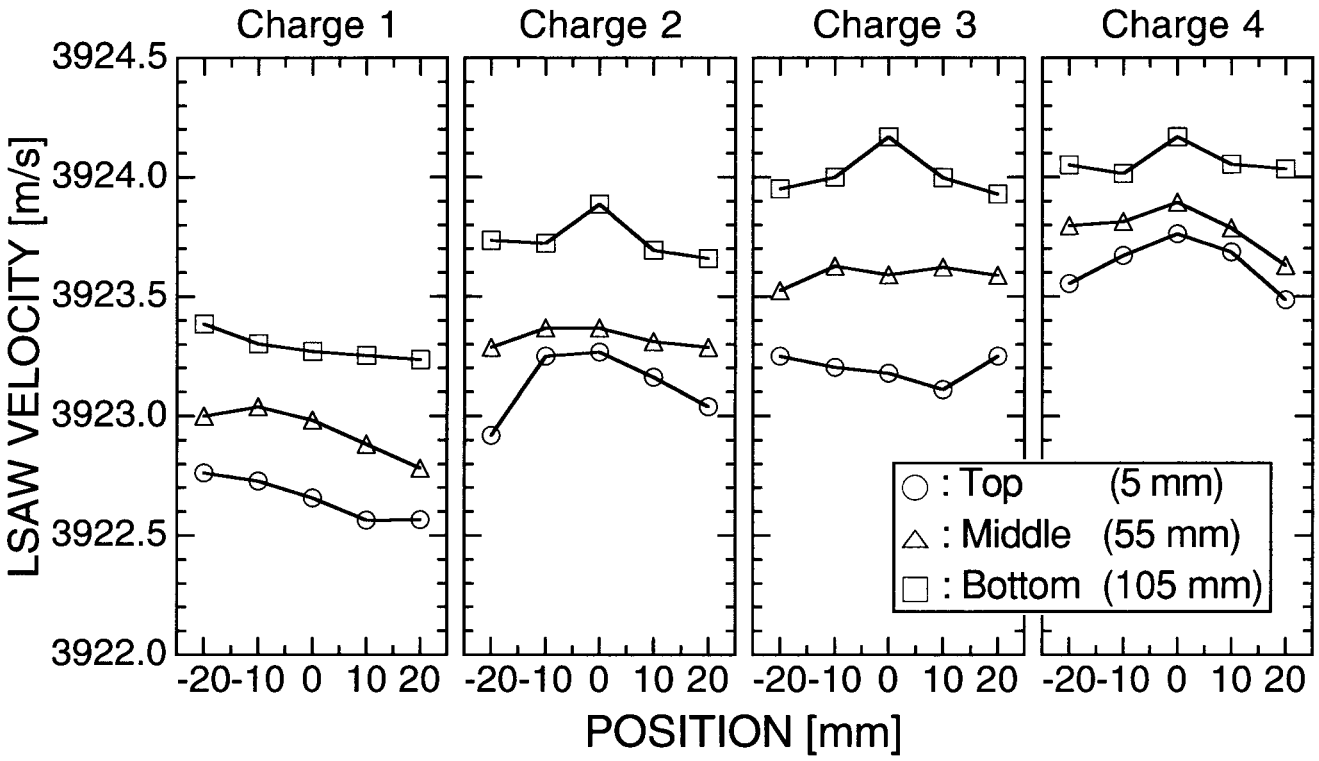

Fig. 5. LSAW velocity distributions for 128°YX-$LiNbO_3$ wafers prepared from a series of four single crystals.

material of the same composition as the decreased amount after each crystal was pulled [4]. Four $LiNbO_3$ single crystals about 115 mm in length and seven $LiTaO_3$ single crystals about 60 mm in length were pulled along the 128°Y axis and along the X axis. Wafers were taken from the top, middle, and bottom parts of each crystal ingot, cut perpendicular to the pulling axis of the crystals as shown in Fig. 4. The 0.5-mm thick 128°Y-cut $LiNbO_3$ wafers were taken at the wafer positions of 5, 55, and 105 mm from the crystal head of each boule. The 0.37-mm thick X-cut $LiTaO_3$ wafers were taken at the 7, 31, and 46 mm positions. The back surface of each wafer is roughened with grinding powder; #600 grinding powder was used for $LiNbO_3$ wafers, and #180 for $LiTaO_3$ wafers.

B. Results

Measurements were made at five positions on each wafer in 10-mm steps over a distance of ±20 mm along a diameter. The LSAW velocities were measured for the X-axis propagation of the 128° Y-cut $LiNbO_3$ wafers and for the exact 112.2° Y-axis propagation of the X-cut $LiTaO_3$ wafers. The RF pulse width was set at 500 ns. Using V_ℓ = 7159 m/s along the 128° Y axis for the $LiNbO_3$ wafers and V_ℓ = 5589 m/s along the X axis for the $LiTaO_3$ wafers as the velocities of longitudinal waves [23], the minimum thicknesses of the specimens to satisfy (1) were h = 1.79 mm for the $LiNbO_3$ wafers and h = 1.40 mm for the $LiTaO_3$ wafers. As the wafer thicknesses for the $LiNbO_3$ wafers are about 0.5-mm thick, and for the $LiTaO_3$ wafers they are about 0.37-mm thick, the back reflection effects are basically present for both groups of wafers. A (111) gadolinium gallium garnet (GGG) standard specimen [22] was used for the system calibration.

1. 128° Y-cut $LiNbO_3$ Crystals: In measuring the 128°YX $LiNbO_3$ wafers, apparent velocity changes with a maximum of about 3 m/s were observed as shown by the solid line in Fig. 2. Therefore, this back reflection influence was eliminated using the moving average processing method [15], [16], [18]. Fig. 5 shows the LSAW velocity distributions in each wafer. The results were obtained for wafers taken from the top (circles), middle (triangles), and bottom (squares) parts of each crystal boule. The results in Fig. 5 indicate that the LSAW velocities increase in each crystal for the wafer positions closer to the bottom of the boule, and that the velocities increase with the number of charges. The velocity variations in each wafer are within 0.35 m/s (0.009 %) for all the wafers. However, the velocity variations along the crystal pulling axis are relatively larger, and the maximum deviation is 1.06 m/s (0.027%) for the charge-3 crystal.

Fig. 6 presents the LSAW velocity averaged over the velocities at the five positions on each wafer in Fig. 5. Averaged velocities are given by circles for the top, by triangles for the middle, and by squares for the bottom wafers of the crystals. The LSAW velocities increase as the wafer positions near the bottom of the crystals and as the charge number increases. As seen from Fig. 6, the LSAW velocity increases from top to bottom of each crystal range from 0.44 to 0.81 m/s (from 0.011 to 0.021%), and the maximum velocity change among all the wafers is 1.41 m/s (0.036%).

2. X-cut $LiTaO_3$ Crystals: The frequency dependences of the LSAW velocities measured for the X-112°Y $LiTaO_3$ wafers are shown by the solid line in Fig. 7. The results for a 3-mm thick specimen, on which there is no back reflection effect, are shown by the dotted line in Fig. 7. The X-112°Y $LiTaO_3$ wafers, which have small back reflection waves due to the relatively large impedance and the roughened back surfaces, have apparent changes of approximately 0.3 m/s. Consequently, we also eliminated the back reflection influence for these measurements using the moving average processing method [15], [16], [18] as done in the preceding measurement. Fig. 8 shows the velocity distributions in each X-112°Y $LiTaO_3$ wafer. The results for the wafers were taken from the top (circles), middle (triangles), and bottom (squares) parts of the crystals. The results in Fig. 8 are similar to the results observed for the $LiNbO_3$ crystals: the LSAW velocities increase as the charge number increases. In addition, relatively large velocity changes [1.3 to 2.5 m/s (0.039-0.077%)] were observed in the wafers taken from the top and middle parts of the charge-1 crystal boule. These changes may reflect some problems during the poling process [8], [9]. In the wafers taken from charges 2 to 7, the maximum velocity change in each wafer was 0.41 m/s (0.012%), and the velocity changes in each crystal were relatively small, with a maximum deviation of 0.50 m/s (0.015%). The changes in the charge-2 crystal, in particular, were very small and uniform, being 0.22 m/s (0.007%).

Fig. 9 shows the LSAW velocity averaged over the velocities at the five positions in each wafer shown in Fig. 8. Averaged velocities are given by circles for the top, by triangles for the middle, and by squares for the bottom wafers of the crystals. Fig. 9 also shows that the LSAW velocities tend to be the largest in the bottom parts of the crystals, and that the LSAW velocities tend to increase as the charge number increases. In Fig. 9, the LSAW velocity increases from the top to the bottom wafers in each crystal, except for the velocities from charge-1 crystal, was 0.04 m/s (0.001%) to 0.34 m/s (0.010%), and the maximum velocity change among those wafers was 1.14 m/s (0.035%). Although the velocity changes between the top and bottom parts of the crystals in the X-112°Y $LiTaO_3$ crystals are less than those in the 128°YX $LiNbO_3$ crystals; these differences are considered to be attributed to the different wafer positions for the two groups of crystals grown with the different crystal growth conditions and different crystal lengths.

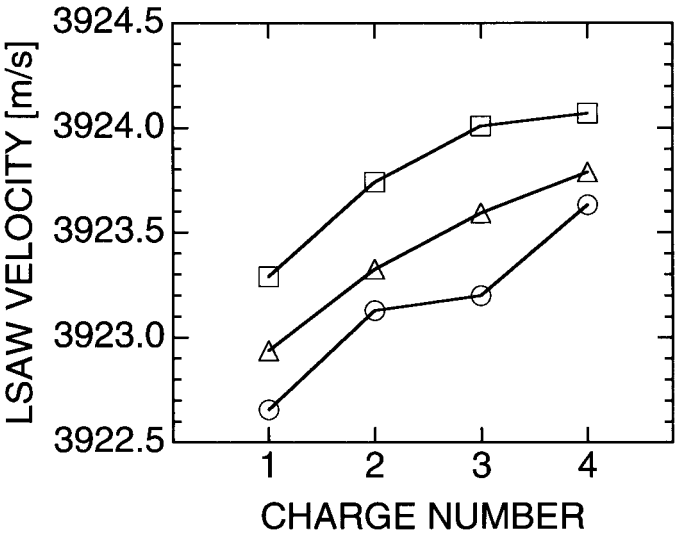

Fig. 6. Relationship between the charge number of crystal growth and averaged LSAW velocities for each 128°YX-$LiNbO_3$ wafer. The results are for wafers prepared from the top (circles), middle (triangles), and bottom (squares) parts of the crystals.

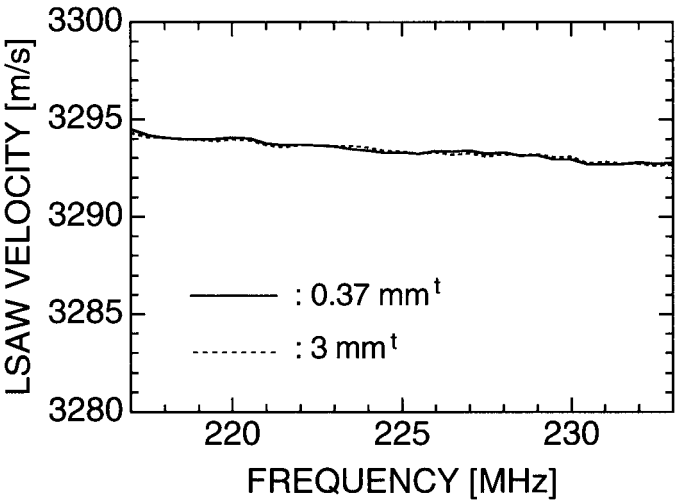

Fig. 7. Frequency dependences of LSAW velocities for X-112° Y $LiTaO_3$ substrates.

C. Discussions

1. Curie Temperature: The LSAW velocity changes (elastic inhomogeneity) in single-domain $LiNbO_3$ and $LiTaO_3$ crystals are basically due to changes in chemical composition [4], [10], [12], [24]. The relationship between the chemical composition ratios and LSAW velocities for the 128°YX $LiNbO_3$ substrates was clarified in the literature [10]. Here, we measured Curie temperatures, which are closely related to the chemical compositions, to investigate the relationship between the chemical composition ratios and LSAW velocities for the $LiTaO_3$ single crystal wafers. Fig. 10 shows the Curie temperatures measured for the top and bottom wafers of each $LiTaO_3$ single crystal by the differential thermal analysis (DTA) method plotted against the averaged LSAW velocities of each top and bottom wafer given in Fig. 9. Circles represent the results for the top wafers, and dots represent those for the bottom wafers. The LSAW velocity is linearly proportional to the Curie temperature in the measurement range. The deviations observed are considered to be due to the large Curie temperature measurement errors (±1°C); those of the LSAW velocities are within ±0.1 m/s. The solid line in Fig. 10 is the approximated line for the results represented by the circles and dots, and its slope is 0.40 (m/s)/°C. The

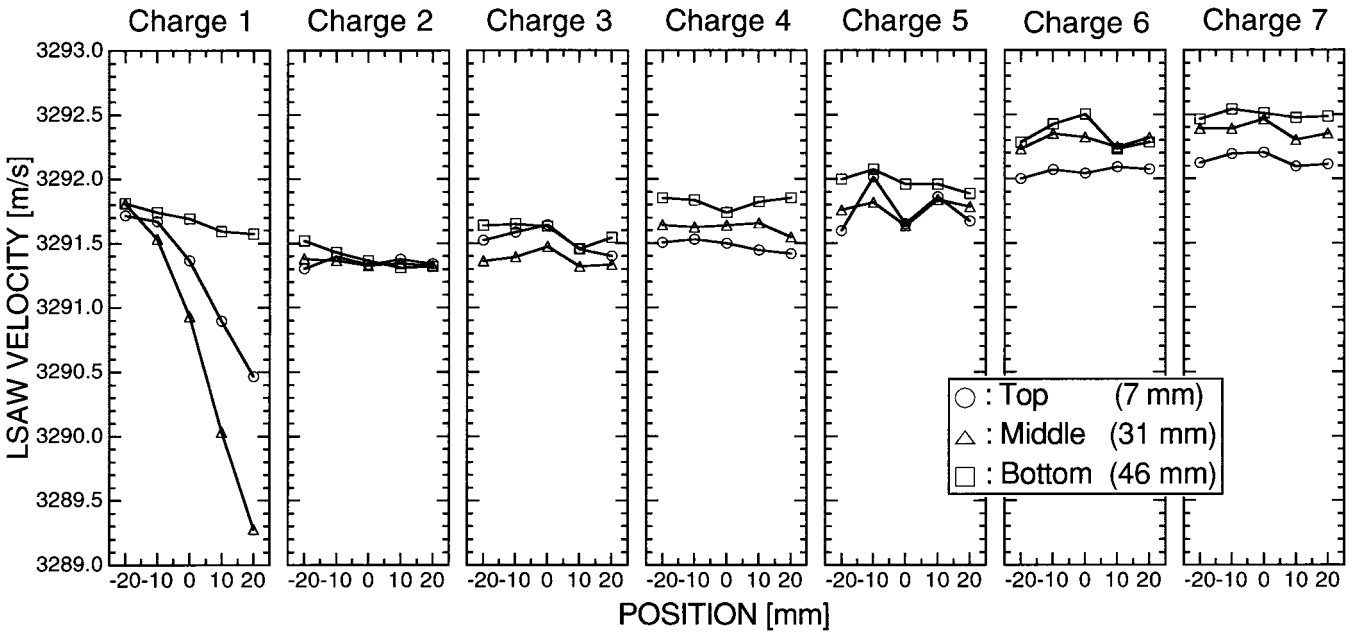

Fig. 8. LSAW velocity distributions for X-112°Y $LiTaO_3$ wafers prepared from a series of seven single crystals.

results suggest that the LSAW velocity changes observed in Figs. 8 and Fig. 9 reflect changes in chemical composition.

2. Chemical Composition Distributions: As seen in Figs. 6 and 9, the maximum velocity change among the 128°YX $LiNbO_3$ wafers was 1.41 m/s, and that among the X-112°Y $LiTaO_3$ wafers, excluding the velocity changes for charge-1 wafers, was 1.14 m/s. Therefore, these velocity changes are converted into changes of chemical compositions. When converted using 0.0269 Li_2O-mol%/(m/s), the relationship between the chemical compositions and LSAW velocities for the 128°YX $LiNbO_3$ substrates in the literature [10], the LSAW velocity change of 1.41 m/s corresponds to a variation of 0.038 Li_2O-mol%. Similarly, for the X-112°Y $LiTaO_3$ substrates, the velocity change of 1.14 m/s corresponds to a variation of 0.075 Li_2O-mol%, from 0.0658 Li_2O-mol%/(m/s) (the relationship between the chemical compositions and LSAW velocities), obtained using 0.0263 Li_2O-mol%/°C (the relationship between the Curie temperature and the chemical composition ratio estimated from the values in the literature [24], [25]) and the slope of 0.40 (m/s)/°C in Fig. 10. The Li_2O concentrations in both series of crystals increased with distance from the head of the crystal and with the charge number. This means that the compositions of the starting materials for $LiNbO_3$ and $LiTaO_3$ crystals used in this study differed slightly from the true congruent compositions. As previously discussed for the development of optical-grade $LiTaO_3$ crystals [25], more homogeneous crystals could be obtained with the Li_2O contents in the starting materials less by about 0.02 mol% for $LiNbO_3$, using the LSAW velocity data for the first 128°YX $LiNbO_3$ crystal, and less by about 0.01 mol% for $LiTaO_3$, using the data for the second X-112.2°Y $LiTaO_3$ crystal, under the same other growth conditions.

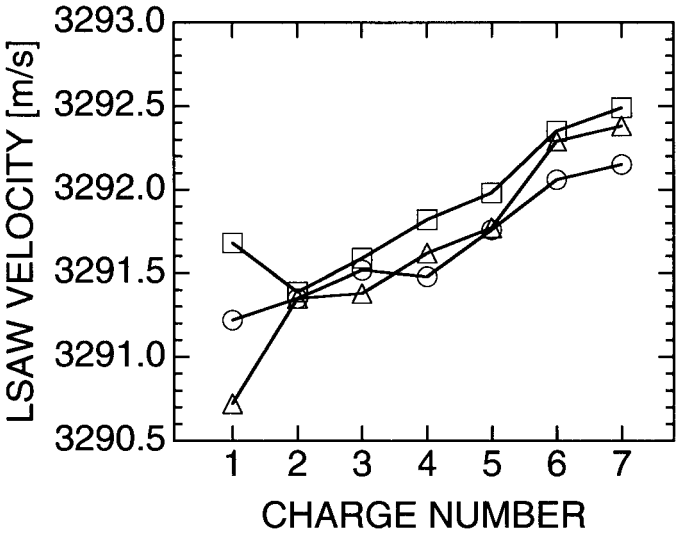

Fig. 9. Relationship between the charge number of crystal growth and averaged LSAW velocities for each X-112°Y $LiTaO_3$ wafer. The results are for wafers prepared from the top (circles), middle (triangles), and bottom (squares) parts of the crystals.

Further details of the velocity distributions for the three wafers of the charge-1 crystal shown in Fig. 8 were investigated. The LSAW velocities were carefully measured in 5-mm steps for an area of 80 mm^{ϕ} to obtain two-dimensional LSAW velocity distributions for two LSAW propagation directions along the 112.2°Y and 22.2°Y axes, in which the usual measurement practice having an RF pulse width of 500 ns was chosen because there is only a very small back reflection effect. Fig. 11 shows the velocity distributions observed on the middle wafer, in which the area was segmented into 5 mm × 5 mm sections. The LSAW velocities were measured at the center of the squares. Relatively large changes for either propagation direction are clearly

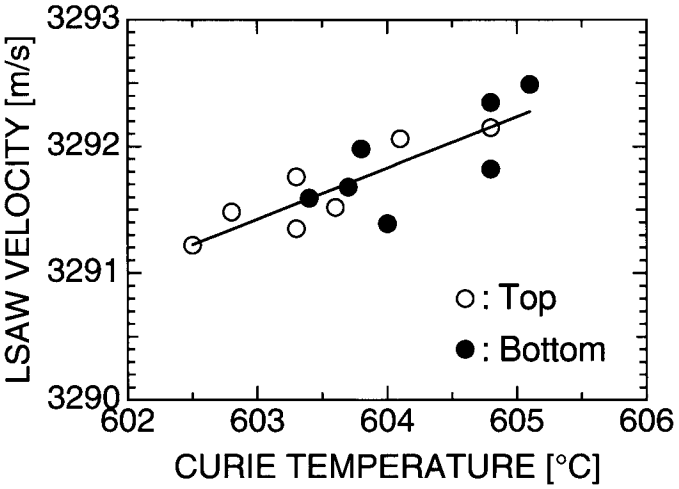

Fig. 10. Relationship between the Curie temperatures and LSAW velocities for X-112°Y $LiTaO_3$. Solid line indicates the approximated line.

observed with a local minimum around (+20, −5) in the half part of the wafer along the crystallographic $+Z$ axis. The maximum velocity differences are 2.9 m/s (0.088%) in the 112.2°Y direction and 1.6 m/s (0.051%) in the 22.2°Y direction. Assuming that these differences are caused by the chemical composition changes, we can estimate that the 2.9 m/s in the 112.2°Y direction and the 1.6 m/s in the 22.2°Y direction correspond to 0.183 Li_2O-mol% and 0.069 Li_2O-mol%, respectively, using the data for the relationships between the LSAW velocities and Li_2O contents in the literature [25]. This trial resulted in the different Li_2O content distributions for the two LSAW propagation directions, so we failed to explain the velocity changes based on the chemical composition changes.

D. Evaluation and Selection

The specimens used in the measurements were produced 10 years ago. At that time, the permissible SAW velocity deviations in crystals and wafers were within ±0.1% for SAW filters and within ±0.04% for resonators operating at not so high frequencies (mostly less than 100 MHz) [4]. From these measured results, the crystals/wafers are good for both filters and resonators, with the exception of charge-1 X-112°Y $LiTaO_3$ crystal. However, the relatively large LSAW velocity variations, 2.6 to 2.9 m/s, were observed in the wafers taken from the top and middle parts of the charge-1 X-112°Y $LiTaO_3$ crystal. A previous report [9] noted that the LSAW velocity for X-112°Y $LiTaO_3$ in the single-domain state is about 85 m/s less than that for X-112°Y $LiTaO_3$ in the multidomain state. The velocity changes associated with the residual multidomain are thus considerably larger than those associated with the chemical composition (about 0.5 m/s in a congruent crystal as experimentally demonstrated in Fig. 8). This implies that the relatively large velocity variations reflect the position dependence of the acoustical physical constants associated with serious polarization problems during the poling process [9], [24], [26], [27], indicating undesirable conditions in the wafer fabrication processes for the crystal. However, in the measured results obtained here, the velocities decreased around the positions poling processed under the undesired conditions. The acoustic properties are quite different from the acoustic property in the multidomain, perfectly depoled crystal [26], [27]. Further investigations will be required to interpret these interesting results. However, it is judged from this discussion that the charge-1 X-cut $LiTaO_3$ crystal having such LSAW velocity variations should not be used for substrates of SAW devices.

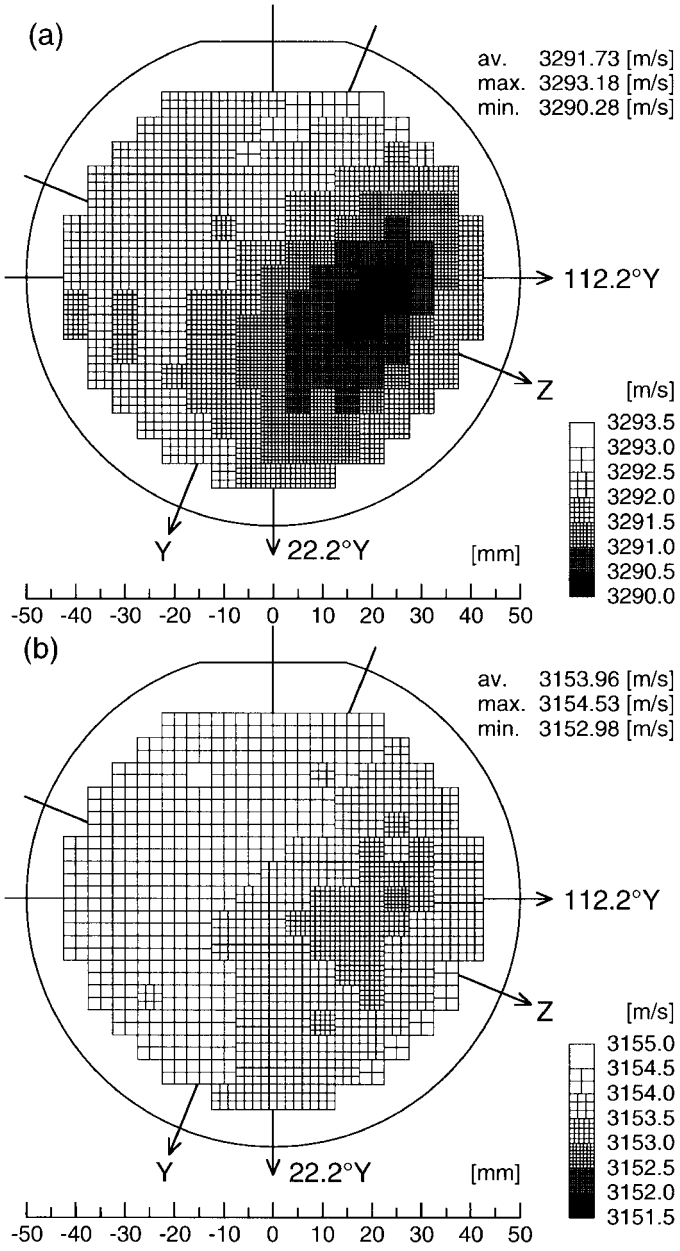

Fig. 11. LSAW velocity distributions measured on the middle-part wafer of the charge-1 X-cut $LiTaO_3$ crystal. (a) 112.2°Y LSAW propagation; (b) 22.2°Y LSAW propagation.

Although the serious problems due to the undesired poling processes detected here sometimes happened in industry more than 10 years ago; these problems have, we be-

lieve, been empirically and completely resolved. However, such variations in elastic properties among crystals and wafers due to slight chemical composition changes (as detected through the evaluation of the specimens used here) still exist at present, even in commercially produced crystals as the conventional techniques do not have the high resolution of this ultrasonic method [10], [11], [25]. Stricter requirements for homogeneity in crystals and wafers are anticipated, particularly for the future mass production of high-performance devices operating at higher frequencies (> 2 GHz).

V. Summary

Several wafer specimens prepared in the industrial production line for SAW devices were evaluated and selected as a practical application of the LFB acoustic microscopy system developed for efficient and highly accurate material characterization. Back reflection causes measurement errors when this system is applied to thin specimens such as wafers, so a measurement procedure including the methods for eliminating the back reflection influence was presented. The system was applied to commercially available $LiNbO_3$ and $LiTaO_3$ single crystals and wafers, and a series of systematic elastic changes among the crystals and wafers was detected for the first time. Furthermore, inhomogeneities in the crystals were detected with a high degree of accuracy, which was nearly impossible with other conventional methods. Based on the measured results, this LFB-UMC system was proved not only to be a promising tool for selecting wafers but also for contributing to the growth of more homogeneous crystals by detecting slight changes in elastic properties among crystals and wafers, and by feeding back the obtained information to improve the crystal growth conditions. This system could be an extremely useful technology for resolving various problems of electronic materials and device fabrication processes in science and industry in the near future.

Acknowledgment

The authors are grateful to I. Sahashi and T. Sasamata of Yamaju Ceramics Co. for supplying the specimens and measuring the Curie temperatures.

References

[1] A. A. Ballman, "Growth of piezoelectric and ferroelectric materials by the Czochralski technique," *J. Amer. Ceram. Soc.*, vol. 48, pp. 112–113, Feb. 1965.

[2] J. R. Carruthers, G. E. Peterson, M. Grasso, and P. M. Bridenbaugh, "Nonstoichiometry and crystal growth of lithium niobate," *J. Appl. Phys.*, vol. 42, pp. 1846–1851, Apr. 1971.

[3] S. Miyazawa and H. Iwasaki, "Congruent melting composition of lithium metatantalate," *J. Cryst. Growth*, vol. 10, pp. 276–278, 1971.

[4] K. Yamada, T. Omi, S. Matsumura, and T. Nishimura, "Characterization of 4-inch $LiTaO_3$ single crystals for SAW device application," in *Proc. IEEE Ultrason. Symp.*, 1984, pp. 243–248.

[5] N. Chubachi, "Ultrasonic micro-spectroscopy via Rayleigh waves," in *Rayleigh-Wave Theory and Application*, E. A. Ash and E. G. S Paige, Eds. New York: Springer-Verlag, 1985, pp. 291–297.

[6] J. Kushibiki and N. Chubachi, "Acoustic microscopy for materials characterization," in *Ultrasonics International 91 Conference Proceedings*, Oxford: Butterworth and Heinemann, 1991, pp. 1–13.

[7] J. Kushibiki and N. Chubachi, "Material characterization by line-focus-beam acoustic microscope," *IEEE Trans. Sonics Ultrason.*, vol. SU-32, pp. 189–212, Mar. 1985.

[8] J. Kushibiki, H. Asano, T. Ueda, and N. Chubachi, "Application of line-focus-beam acoustic microscope to inhomogeneity detection on SAW device materials," in *Proc. IEEE Ultrason. Symp.*, 1986, pp. 749–753.

[9] J. Kushibiki, H. Takahashi, T. Kobayashi, and N. Chubachi, "Quantitative evaluation of elastic properties of $LiTaO_3$ crystals by line-focus-beam acoustic microscopy," *Appl. Phys. Lett.*, vol. 58, pp. 893–895, Mar. 1991.

[10] J. Kushibiki, H. Takahashi, T. Kobayashi, and N. Chubachi, "Characterization of $LiNbO_3$ crystals by line-focus-beam acoustic microscopy," *Appl. Phys. Lett.*, vol. 58, pp. 2622–2624, June 1991.

[11] J. Kushibiki, T. Kobayashi, H. Ishiji, and N. Chubachi, "Elastic properties of 5-mol % MgO doped $LiNbO_3$ crystals measured by line focus beam acoustic microscopy," *Appl. Phys. Lett.*, vol. 61, pp. 2164–2166, Nov. 1992.

[12] J. Kushibiki, H. Ishiji, T. Kobayashi, N. Chubachi, I. Sahashi, and T. Sasamata, "Characterization of 36°YX-$LiTaO_3$ wafers by line-focus-beam acoustic microscopy," *IEEE Trans. Ultrason., Ferroelect., Freq. Contr.*, vol. 42, pp. 83–90, Jan. 1995.

[13] T. Kobayashi, J. Kushibiki, and N. Chubachi, "Improvement of measurement accuracy of line-focus-beam acoustic microscope system," in *Proc. IEEE Ultrason. Symp.*, 1992, pp. 739–742.

[14] J. Kushibiki, Y. Ono, and I. Takanaga, "Ultrasonic microspectroscopy of $LiNbO_3$ and $LiTaO_3$ single crystals for SAW devices," *IEICE Trans. Electron.*, vol. J82-C-I, pp. 715–727, Dec. 1999.

[15] J. Kushibiki, Y. Ohashi, and M. Arakawa, "Precise velocity measurements for thin specimens by line-focus-beam acoustic microscopy," *Jpn. J. Appl. Phys.*, vol. 38, pp. L89–L91, 1999.

[16] J. Kushibiki and Y. Ohashi, "Theoretical and experimental considerations on line-focus-beam acoustic microscopy for thin specimens," *Jpn. J. Appl. Phys.*, vol. 38, pp. L342–L344, 1999.

[17] Y. Ohashi and J. Kushibiki, "Correction of velocity profiles on thin specimens measured by line-focus-beam acoustic microscopy," *Jpn. J. Appl. Phys.*, vol. 38, pp. L1197–L1200, Oct. 1999.

[18] J. Kushibiki, Y. Ohashi, and M. Arakawa, "Influence of reflected waves from the back surface of thin solid-plate specimen on velocity measurements by line-focus-beam acoustic microscopy," *IEEE Trans. Ultrason., Ferroelect., Freq. Contr.*, vol. 47, pp. 274–284, Jan. 2000.

[19] K. Shibayama, K. Yamanouchi, H. Sato, and T. Meguro, "Optimum cut for rotated Y-cut $LiNbO_3$ crystal used as the substrate of acoustic-surface-wave," in *Proc. IEEE*, vol. 64, pp. 595–597, May 1976.

[20] H. Hirano, T. Fukuda, S. Matsumura, and S. Takahashi, "$LiTaO_3$ single crystals for SAW device applications: (1) Characteristics of the material," *Proc. 1st Meeting on Ferroelectric Materials and Their Applications*, Kyoto, Japan, 1978, pp. 81–86.

[21] J. Kushibiki and Y. Ono, "Development of the line-focus-beam ultrasonic material characterization system," unpublished.

[22] J. Kushibiki and M. Arakawa, "A method for calibrating the line-focus-beam acoustic microscopy system," *IEEE Trans. Ultrason., Ferroelect., Freq. Contr.*, vol. 45, pp. 421–430, Mar. 1998.

[23] J. Kushibiki, I. Takanaga, M. Arakawa, and T. Sannomiya, "Accurate measurements of the acoustical physical constants of $LiNbO_3$ and $LiTaO_3$ single crystals," *IEEE Trans. Ultrason., Ferroelect., Freq. Contr.*, vol. 46, pp. 1315–1323, Sep. 1999.

[24] M. Sato, A. Iwama, J. Yamada, M. Hikita, and Y. Furukawa, "SAW velocity variation $LiTaO_3$ substrates," *Jpn. J. Appl. Phys.*, vol. 28, Suppl. 28-1, pp. 111–113, 1989.

[25] J. Kushibiki, T. Okuzawa, J. Hirohashi, and Y. Ohashi, "Line-focus-beam acoustic microscopy characterization of optical-

grade $LiTaO_3$ single crystals," *J. Appl. Phys.*, vol. 87, pp. 4395–4403, May 2000.
[26] J. Kushibiki and I. Takanaga, "Elastic properties of single- and multi-domain crystals $LiTaO_3$," *J. Appl. Phys.*, vol. 81, pp. 6906–6910, May 1997.
[27] I. Takanaga and J. Kushibiki, "Elastic constants of multidomain $LiTaO_3$ crystal," *J. Appl. Phys.*, vol. 86, pp. 3342–3346, Sep. 1999.

Jun-ichi Kushibiki (M'83) was born in Hirosaki, Japan, on November 23, 1947. He received the B.S., M.S., and Ph.D. degrees in electrical engineering from Tohoku University, Sendai, Japan, in 1971, 1973, and 1976, respectively.

In 1976, he became Research Associate at the Research Institute of Electrical Communication, Tohoku University. In 1979, he joined the Department of Electrical Engineering, Faculty of Engineering, Tohoku University, where he was Associate Professor from 1988 to 1993 and became Professor in 1994. He has been studying ultrasonic metrology, especially acoustic microscopy and its applications, and has established a method of material characterization by LFB acoustic microscopy. He also has been interested in biological tissue characterization in the higher frequency range, applying both bulk and acoustic microscopy techniques.

Dr. Kushibiki is a member of the Acoustical Society of America; the Institute of Electronics, Information, and Communication Engineers of Japan; the Institute of Electrical Engineers of Japan; the Acoustical Society of Japan; and the Japan Society of Ultrasonics in Medicine.

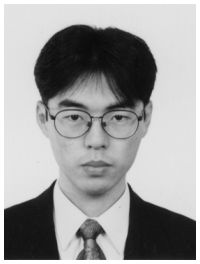

Yuji Ohashi was born in Toyama Prefecture, Japan, on August 27, 1973. He received the B.S. and M.S. degrees in electrical engineering from Tohoku University, Sendai, Japan, in 1996 and 1999, respectively.

He is currently studying toward the Ph.D. degree at Tohoku University. His research interests include development of LFB acoustic microscopy system and its applications to materials characterization.

Mr. Ohashi is a member of the Acoustical Society of Japan.

Yuu Ono (M'99) was born in Yamanashi Prefecture, Japan, March 18, 1967. He received the B.S., M.S., and Ph.D. degrees in electrical engineering from Tohoku University, Sendai, Japan, in 1990, 1992, and 1995, respectively.

Since 1995, he has been a research associate at the Department of Electrical Engineering, Faculty of Engineering, Tohoku University. He has been studying the development of the line-focus-beam acoustic microscopy system and its application to material characterization.

Dr. Ono is a member of the Institute of Electronics, Information and Communication Engineers of Japan; the Acoustical Society of Japan; the Japan Society of Applied Physics, and IEEE.